HHS Public Access

Author manuscript

Sci Immunol. Author manuscript; available in PMC 2019 January 20.

Published in final edited form as:

Sci Immunol. 2018 July 20; 3(25): . doi:10.1126/sciimmunol.aas9103.

TCR signal strength controls the differentiation of CD4+ effector and memory T cells

Jeremy P. Snook[1], **Chulwoo Kim**[2], and **Matthew A. Williams**[1,*]

[1]Department of Pathology, University of Utah School of Medicine, Salt Lake City, Utah 84112.

[2]Department of Medicine, Stanford University School of Medicine, Stanford, California 94305.

Abstract

CD4+ T cell responses are composed of heterogeneous TCR signals that influence the acquisition of effector and memory characteristics. We sought to define early TCR-dependent activation events that control T cell differentiation. A polyclonal panel of TCRs specific for the same viral antigen demonstrated substantial variability in TCR signal strength, expression of CD25 and activation of NFAT and NFκB. Following viral infection, strong TCR signals corresponded to Th1 differentiation, whereas Tfh and memory T cell differentiation were most efficient when TCR signals were comparatively lower. We observed substantial heterogeneity in TCR-dependent CD25 expression *in vivo*, and the vast majority of CD4+ memory T cells were derived from CD25lo effector cells that displayed decreased TCR signaling *in vivo*. Nevertheless, memory T cells derived from either CD25lo or CD25hi effector cells responded vigorously to rechallenge, indicating that while early clonal differences in CD25 expression predicted memory T cell numbers, they did not predict memory T cell function on a per cell basis. Gene transcription analysis demonstrated expression clustering based on CD25 expression and enrichment of transcripts associated with enhanced Tfh and memory development within CD25lo effector cells. Direct enhancement of TCR signaling via knockdown of SHP-1, a tyrosine phosphatase that suppresses early TCR signaling events, favored the differentiation of Th1 effector and memory cells. We conclude that strong TCR signals during early T cell activation favor terminal Th1 differentiation over long-term Th1 and Tfh memory responses.

One Sentence Summary:

Strong TCR signals favor the differentiation of short-lived effector Th1 cells over long-lived memory T cells.

*Correspondence: M.A. Williams; matthew.williams@path.utah.edu.

Author contributions

J. Snook, C. Kim and M. Williams formulated the experimental design and performed major experiments and data analysis. J. Snook performed statistical analysis. J. Snook and M. Williams wrote and revised the manuscript and conceptualized results.

Competing Interests

The authors declare no competing financial interests.

Data and Materials Availability

Sequencing data has been placed in the GEO repository (GSE114884).

Introduction

The induction of memory T cells is a key focus in the development of vaccines and immunotherapies directed towards infectious pathogens and tumors (1, 2). The primary T cell response to acutely infecting pathogens is marked by rapid proliferation and the development of key effector functions. Following pathogen clearance, 90–95% of effector T cells die, leaving behind a long-lived population of memory T cells (3, 4). $CD8^+$ effector T cells that are memory precursors can be identified by the expression of cell surface markers such as IL-7Rα (5), and some progress has been made in identifying memory-precursor $CD4^+$ T cells (6). However, the specific signals and mechanisms that dictate $CD4^+$ memory T cell fate commitment during the effector response remain elusive.

External differentiation cues, such as cytokines, play a well-known role in controlling T helper subset effector and memory differentiation. However, cell-intrinsic signals mediated by the TCR also control many aspects of $CD4^+$ T cell differentiation. $CD4^+$ T cells require multiple interactions with their cognate antigen to successfully differentiate into competent effector (7, 8) and memory (9) T cells. Several lines of evidence indicate that strong TCR signals favor Th1 differentiation both *in vitro* (10) and *in vivo* (11). Additionally, Th1 differentiation is associated with enhanced CD25 expression (12), an early activation marker driven by TCR signaling. In contrast, Tfh specification has been associated, in separate studies, with high affinity TCRs or TCRs with long dwell times (13, 14), and occupation of multiple ITAMs on a single CD3ζ is also required for Tfh differentiation (15). Monoclonal T cell populations responding to the same epitope can also produce heterogeneous TCR signals, leading to differential effector fates (11, 12). The TCR-dependent early activation genes IL-2 and IL-2Rα (CD25) are also implicated in T helper differentiation. Exogenous IL-2 treatments (16) or analysis of early CD25 expression profiles (12) have highlighted a key temporal role for IL-2 signaling in T helper differentiation. A key downstream transcription factor of IL-2 signaling, STAT5, has been shown to drive Th1 development (17), and IL-2 and IL-21 have been shown to promote Th1 and Tfh differentiation, respectively, although it is not clear whether the effect is paracrine or autocrine (18, 19).

Because TCR molecules are themselves highly variable, the antigen-specific response to an infection is marked by a high level of clonal diversity (20, 21). However, this diversity is subject to a process of selection as shown by our previous finding that not all T cell clones give rise to memory cells with equal efficiency following acute infection with lymphocytic choriomeningitis virus (LCMV) or *Listeria monocytogenes* (Lm) (22). The goal of the current study is to acquire a better understanding of the TCR signals propagated by "memory-biased" versus "effector-biased" T cell clones during the polyclonal response.

We analyzed a panel of previously cloned TCRs, all recognizing the same MHC Class II-restricted epitope, $GP_{61–80}$ of LCMV, and each with a previously defined contribution to the $CD4^+$ memory T cell pool during an *in vivo* polyclonal response. We found that overall TCR signal strength inversely corresponded to the contribution of each TCR to the formation of T cell memory. During *in vivo* infection with LCMV, the extent of both ZAP-70 phosphorylation and CD25 expression at early effector time points inversely corresponded to memory potential. Heterogeneous CD25 expression predicted a bias in the formation of Th1

and Tfh populations. $CD25^{lo}$ effector cells gave rise to a mix of Th1 and Tfh effector cells, as well as most Th1-like and Tfh-like memory cells, whereas $CD25^{hi}$ early effector cells gave rise almost exclusively to terminally differentiated effector Th1 cells. This differential T cell fate was further supported through global transcriptional analysis. Direct modulation of TCR signaling via the shRNA-mediated knockdown of the tyrosine phosphatase SHP-1 additionally biased the response towards the differentiation of effector Th1 cells, indicating that TCR signal strength shapes the differential formation of both effector and memory $CD4^+$ T cells with Tfh or Th1 characteristics.

Results

Heterogeneous induction of TCR signals in vitro corresponds to in vivo fate

We investigated a panel of natively arising TCRs specific for the immunodominant MHC Class II-restricted epitope of LCMV, $GP_{61–80}$ (Fig. S1A). All TCRs in the panel were derived from SMα mice, single chain TCR transgenic mice expressing the TCRα of the SMARTA TCR ($GP_{61–80}$-specific) paired to an endogenous TCRβ repertoire (20). Because each cloned TCR has a defined contribution to memory in the setting of *in vivo* viral infection (20), we employed this panel to assess the consequences of differential signaling initiated by "memory-biased" and "effector-biased" TCRs. We first created cell lines expressing each TCR by transducing a parent hybridoma T cell line with recombinant retroviruses expressing a bicistronic TCR construct and a mCherry reporter (Fig. S1B) (23). The parent hybridoma line did not express an endogenous TCR and contained a GFP reporter under the control of a minimal consensus NFAT-sensitive promoter (24). We further transduced each hybridoma line with an additional retrovirus containing a cyan fluorescent protein (CFP) reporter under the control of an NFκB response element (25), thus allowing us to simultaneously detect NFAT and NFκB activity (Fig. S1B). Each line expressed similar levels of surface TCR (Fig. S1A) and GFP following stimulation with PMA/ionomycin (Fig. 1A). Hybridomas were co-incubated for 24 hours with dendritic cells presenting $GP_{61–80}$ peptide on MHC Class II (pepDC). GFP production by each hybridoma cell line was measured by flow cytometry (Fig. 1A) and confirmed by Western blot (Fig. S1C). The TCR-dependent NFAT activity, as measured by GFP induced by each cell line, was highly heterogeneous and inversely corresponded to our previous assessment of the memory potential of each TCR (Fig. 1A-B, Fig. S1C). TCRs previously shown to have lower representation in the memory compartment, as compared to the peak of the effector response (Mem^{Lo}, Fig. S1A), induced significantly higher levels of GFP than TCRs previously shown to have equal or higher representation in the memory compartment, as compared to the peak of the effector response (Mem^{Hi}, Fig. S1A). Similar results were found when we assessed NFκB-induced CFP expression (Fig. 1B). We also measured TCR-dependent gene expression. After 24 hours of stimulation, induction of CD25 surface expression corresponded to GFP expression (Fig. 1C).

To further explore differences in TCR signaling in the context of primary T cell activation, we created two transgenic mouse lines expressing TCRs that recognize $GP_{61–80}$ of LCMV (C7 and C26). C7 $CD4^+$ T cells displayed diminished phosphorylation of ZAP-70 and CD3ζ after 1 hour of co-incubation with pepDCs, as compared to C26 cells (Fig. S2A-B).

Additionally, C7 T cells expressed lower levels of the TCR-dependent activation marker CD25 than C26 T cells after 24 hours of stimulation (Fig. S2C). We also performed RT-PCR on RNA extracted from C7 or C26 splenocyte cultures that had been stimulated with 0.1 μM $GP_{61–80}$ for 1 to 3 days, with particular focus on genes immediately upregulated following TCR activation (*Il2*, *Nfatc1*) or involved in effector function (*Tbx21*, *Ifng*). C26 T cells demonstrated increased expression of *Nfatc1* and *Il2* by day 3 of culture (Fig. S2D). C26 T cells also expressed higher levels of *Ifng* and *Tbx21* transcripts at days 1 and 3 of culture (Fig. S2D). Prior studies have suggested that strong TCR signals promote enhanced Th1 differentiation, and our findings are consistent with that premise (11, 26). These findings confirm heterogeneous TCR signaling and TCR-dependent activation induced by two TCRs that recognize the same immunodominant epitope.

Inter-clonal differences in TCR signal strength and CD25 expression predict effector and memory differentiation

In our previous studies, we utilized SMα mice to establish a role for the TCR in regulating $CD4^+$ memory T cell differentiation. We observed that "memory-biased" TCRs (represented at higher frequencies at memory time points than at effector time points) were enriched for $V\beta14^+$ T cells, whereas "effector-biased" TCRs (represented at higher frequencies at effector time points than at memory time points) were enriched for $V\beta7^+$ T cells (20). We took advantage of this observation in order to assess the expression of CD25 on effector T cells that were more or less likely to give rise to memory T cells. We infected SMα mice with LCMV, followed by detection of $GP_{66–77}$ tetramer-binding $CD4^+$ T cells in the spleen at day 5 post-infection. We found that responding $V\beta14^+$ effector cells were less likely to express CD25 than the tetramer binding population as a whole, while $V\beta7^+$ effector cells were more likely to express CD25 (Fig. 2A). T-bet expression was also higher in the $V\beta7^+$ effector cells (Fig. 2B), leading to the conclusion that within a monoclonal population $CD25^{lo}$ effector cells were more likely to give rise to memory T cells, whereas $CD25^{hi}$ effector cells were enriched for terminally differentiated Th1 cells. We additionally assessed the expression of CD25 in early effector cells derived from a polyclonal T cell repertoire in wildtype mice. At day 5 post-infection, we observed highly variable CD25 expression within activated (IA^b-$GP_{66–77}$ tetramer$^+$, $CD44^+$) $CD4^+$ T cells (Fig. S3), indicating that CD25 expression is broadly heterogeneous during a physiologic T cell response *in vivo*.

We next asked whether clonal differences in TCR signal strength predicted memory formation *in vivo*. We performed a clone-by-clone analysis by generating several TCR retrogenic T cell lines as previously (20, 27, 28)(Fig. S1A), adoptively transferring them into B6 mice and infecting with LCMV one day later. For each of the four clones tested (5, 7, 26, 27) we observed heterogeneity in the phosphorylation of ZAP-70 and the expression of CD25 by day 3 post-infection (Fig. 2C). We further measured the number of peak effector (day 8) and memory cells (day 42) for each clone. We found that reduced expression of phosphorylated ZAP-70 at day 3 in clones 5 and 7, as compared to clones 26 and 27, significantly corresponded to the proportion of resulting peak effector cells that gave rise to memory cells (Fig. 2D). A significantly smaller proportion of clone 5 T cells expressed high levels of CD25 as compared to clones 26 and 27, whereas clone 7 displayed an intermediate

phenotype (Fig. 2C). CD25 also corresponded to memory formation, although in this case the differences indicated a trend only (Fig. 2D).

Differences in CD25 expression correspond to differences in TCR signal strength in vivo

We next employed an adoptive transfer model in which WT mice (Thy1.2$^+$) received an i.v. injection of SMARTA TCR transgenic CD4$^+$ T cells (Thy1.1$^+$), followed by infection with LCMV one day later. SMARTA T cells showed uniform patterns of CD25 expression through day 2 post-infection, with almost all activated T cells expressing high levels of CD25 by day 2. By day 3, however, a proportion of SMARTA T cells expressed low levels of CD25, and this bimodal expression persisted through day 5. We found similar results when assessing the expression of CD25 by C7 and C26 T cells after LCMV infection. Additionally, the proportion of CD25^{lo} early effector cells was significantly different when comparing C7 and C26 at day 3 post-infection (Fig. S4A), similar to the clonal differences in CD25 expression observed for retrogenic T cell clones (Fig. 2). Differences in CD25 expression did not coincide with differences in the expression of classical activation markers CD44 and CD62L or secretion of the effector cytokines IFNγ, TNFα and IL-2 (Fig S4B).

CD25 surface expression predicted differences in effector differentiation. CD25^{hi} early SMARTA effector cells (day 3 post-infection) in the spleen expressed phenotypic markers indicative of Th1 differentiation (Ly6C, Tim-3) that were largely absent on CD25^{lo} effector cells (Fig. 3B). CD25^{hi} SMARTA early effector cells additionally expressed higher levels of T-bet (Fig. 3C), while CD25^{lo} effector cells expressed increased levels of the Tfh markers CXCR5 and TCF-1 (Fig. 3C). Furthermore, CD25^{hi} effector cells in the spleen expressed higher levels of phosphorylated ZAP-70 at days 3 and 5 post-infection (Fig. 3D).

CD25 surface expression predicts memory potential

Given the heterogeneity of TCR signaling and CD25 expression even within monoclonal populations, we tested whether CD25 surface expression by early effector cells predicted effector and memory differentiation. Several lines of evidence suggested this possibility. First, CD25 expression distinguished CD8$^+$ effector T cells likely to undergo terminal effector differentiation from those that give rise to memory T cells (29). Second, Blimp-1 expression by early CD4$^+$ effector T cells inversely corresponded to memory potential, and CD25 was strongly co-expressed with Blimp-1 in those studies (12). Third, *in vitro* induction of CD25 driven by TCR signal strength strongly corresponded to increasing Th1 polarization (Fig. 3C-D, Fig. S2D).

We isolated CD25^{hi} and CD25^{lo} SMARTA effector cells at days 3 or 5 post-infection and transferred them into separate infection-matched B6 hosts in equal numbers (Fig. 4A). While both populations continued to expand, the vast majority of circulating and spleen-residing memory cells were derived from the CD25^{lo} effector population as early as day 3 post-infection (Fig. 4B-C). In contrast, both CD25^{lo} and CD25^{hi} early effector cells gave rise to liver-residing memory T cells (Fig. 4C) with similar efficiency. This may reflect the reported role for IL-2 in the establishment of tissue-residing CD4+ memory T cells (30, 31), although the interpretation is made complex by the temporal changes that we observed in high affinity IL-2R expression (Fig. 3A). We used an additional retrogenic T cell line (clone

18), generated as previously (Fig. S1) to perform similar adoptive transfer experiments. As with SMARTA T cells, CD25^{lo} clone 18 early effector cells similarly gave rise to most memory T cells (Fig. S5A-B), indicating that CD25 expression predicts memory differentiation across multiple clones.

CD25 expression at early effector time points further predicted T helper differentiation at the peak of the effector response (day 8). CD25^{hi} early effector cells gave rise to mostly Th1 cells at day 8 post-infection, as measured by increased expression of Ly6C and Tbet. In contrast, CD25^{lo} cells gave rise to mostly Tfh effector cells at day 8 post-infection, as measured by expression of CXCR5, PD-1 and Bcl-6 (Fig. 4D-E). Similar results were obtained following transfer of CD25^{hi} or CD25^{lo} clone 18 early effector cells (Fig. S5C). Memory cells derived from CD25^{hi} effector cells expressed increased Tbet (Fig. 4F), consistent with the differentiation of effector memory cells. These results indicate a role for TCR signaling in driving both memory and effector CD4^{+} T cell differentiation.

CD25 expression during the primary response does not predict memory T cell function

To test the memory function of CD25^{hi}-derived or CD25^{lo}-derived SMARTA memory cells, we isolated SMARTA cells at day 42 after primary LCMV infection, transferred them into naïve hosts and rechallenged them with LCMV (Fig. 5A). At the peak of their secondary response (d5 post infection), both CD25^{lo}- and CD25^{hi}-derived SMARTA memory cells had undergone similar levels of clonal expansion (Fig. 5B). We observed no differences in secondary Th differentiation, as shown by expression of CXCR5, PD-1, Ly6C, Bcl-6 and Tbet (Fig. 5C-D). We concluded that while CD25^{lo} and CD25^{hi} early effector cells gave rise to different numbers of memory cells, secondary expansion and differentiation of those memory cells was similar. Further, we determined that memory cells were highly functional regardless of whether they were derived from CD25^{hi} or CD25^{lo} effector cells, as shown by high levels of effector cytokine secretion upon *ex vivo* re-stimulation (Fig. 5E).

CD25 expression identifies two transcriptionally distinct subsets of early effector cells

We utilized RNASeq to compare the gene expression profiles of CD25^{hi} and CD25^{lo} SMARTA effector cells undergoing different levels of TCR signaling at day 5 post-infection. Each population had a unique transcriptional signature, as shown by cluster analysis of genes that showed significant differential expression (Fig. 6A). Among these genes was CD25 itself, which indicated that differences in CD25 expression were transcriptionally regulated and served as an internal control for the validity of the analysis (Fig. 6B). CD25^{hi} early effector cells had increased expression of a number of NFAT-inducible genes, including *Runx3* (32), *Ifng* (32) and *Ppp3ca* (33), and other TCR-inducible genes, including *Bhlhe40* (34) and *Dusp22* (35). Furthermore, gene expression in CD25^{hi} cells was indicative of enhanced Th1 differentiation, as determined by expression of *Prf1*, *Il12rb2*, *Tbx21* and *Prdm1* (Blimp-1)(19, 36, 37). *IL12rb2* expression has also been associated with TCR signal strength (38). In contrast, CD25^{lo} effector cells had increased expression of genes related to the regulation of T cell activation such as *Btla* (39), *Egr2* and *Egr3* (40); genes associated with memory T cell formation such as *Tcf7* (TCF-1) (41, 42), *Pou2af1* (OCA-B) (43), and *Cd27* (44); and genes associated with Tfh differentiation such as *Cebpa*, *Tcf7, Il6st*, *Id3* and

Il6ra (Fig. 5B) (18, 41, 45). Differential expression of key genes was confirmed via RT-PCR (Fig. 6C).

Decreased SHP-1, a key TCR signaling modulator, reduces Tfh differentiation

To modulate TCR signal strength in primary $CD4^+$ T cells, we targeted the protein tyrosine phosphatase SHP-1 via shRNA. Because SHP-1 is a key regulator of the activity of TCR proximal tyrosine kinases, including ZAP-70 (46), we hypothesized that SHP-1 knockdown would result in enhanced and/or sustained TCR signaling. We expressed two different mir30-flanked shRNAs in retroviral expression plasmids, both specific for SHP-1, that had been previously described and displayed significant SHP-1 knockdown (30–80%) when expressed in EL-4 cells (Fig. S6A) (47). We then generated bone marrow chimeras by transducing SMARTA bone marrow with SHP-1 shRNA retroviral vectors (SHP-1 KD), or an empty vector control (EV), and transplanting into irradiated $Rag^{-/-}$ recipients. 8–10 weeks later, cells were stimulated *in vitro* with DCs presenting $GP_{61–80}$ and tested for the presence of pZAP-70. For both shRNA constructs, SHP-1 KD resulted in more rapid induction and sustained maintenance of pZAP-70 (Fig. S6B), indicating an impact on TCR signal strength.

GFP^+ (SHP-1 KD or EV) and GFP^- (WT) cells from the chimeras were adoptively transferred into B6 recipient mice, followed by LCMV infection. This allowed us to compare SHP-1 KD and empty vector (EV) SMARTA responses in different hosts as well as responses by transduced (GFP^+) and non-transduced (GFP^-) SMARTA cells in the same host. As early as day 3 post infection, a Th1 bias was present in SHP-1 KD SMARTA cells, evidenced by increased levels of CD25 and Tim3 compared to WT and EV controls (Fig. 7A). SHP-1 KD did not affect the overall activation of the SMARTA $CD4^+$ T cells, as measured by CD44 and CD62L expression (Fig. 7B). Day 8 effector cells also evidenced a Th1 bias, as determined by a decrease in the proportion of effector cells expressing CXCR5 and an increase in the proportion of effector cells expressing Ly6C (Fig. 7C-D). The bias away from Tfh differentiation persisted into memory, as SHP-1 KD resulted in significantly fewer Tfh-like memory cells (Fig. 7C). However, at both effector and memory time points the overall number of SMARTA was not significantly altered by SHP-1 KD, indicating that the decrease in Tfh was compensated by an increase in Th1. In support of this, SHP-1 KD cells produced the Th1 cytokine IFNγ at a higher frequency and an increased level on a per cell basis than their WT counterparts (Fig. 7E). We concluded that effector and memory $CD4^+$ T cell differentiation is governed, at least in part, by TCR signal strength.

Discussion

Our results find a key role for TCR signal strength, as regulated by SHP-1, in determining clonal differences in both T helper differentiation (Th1 vs. Tfh) and memory formation. The TCR has previously been shown to influence T helper cell differentiation (11, 13, 15). Strong TCR signals favor Th1 over Th2 differentiation (11), and the extent of Th1 effector function and polarization is dependent on TCR signal strength (26). The TCR also plays a role in the differentiation of Th1 and Tfh cells. In one study, high affinity TCRs favored the differentiation of Tfh (13), while in a second study Tfh differentiation corresponded to long

TCR/pMHC dwell times (14). More recently, it was found that limiting TCR signaling in T cells selectively impaired Tfh differentiation, while leaving Th1 responses relatively untouched (15). In contrast, our findings demonstrate a correlation of stronger TCR signals and terminal Th1 differentiation, whereas the differentiation of both Tfh and Th1 with memory potential required comparatively weaker TCR signals. Several possibilities may explain these differences. First, while we show that TCR signaling distinguishes terminal effector cells from memory precursors, it is not clear how it might influence the differentiation of Th1 and Tfh derived from $CD25^{lo}$ effector cells. Second, the role of the TCR may be influenced by antigen availability, antigen localization or the infection-dependent inflammatory environment. Third, TCR signaling is unlikely to be uniform throughout the primary response, and the impact of altering TCR signaling may depend on the approach.

IL-2 has been shown to play an important role in the generation of Th1 cells (15) and effector and memory CD4+ memory T cells that home to tertiary organs (30, 31). In contrast to the preferential survival of $CD25^{lo}$ effector T cell in circulation and in secondary lymphoid organs, $CD25^{hi}$ effector cells gave rise to liver-residing memory T cells with equal efficiency to $CD25^{lo}$ effector cells. This may reflect the variable role of IL-2 in driving the formation of these memory populations. It is noteworthy that CD25 is expressed by virtually all T cells during early activation. It is not known if IL-2 signaling is required for tissue-resident memory T cell development only during the early phases of the effector response, or if sustained IL-2 signaling is required throughout the effector response. Given the heterogeneity of the expression of the high affinity IL-2 receptor, it will be of interest to define these differences, and to determine whether the TCR mechanistically controls T cell fate at least in part by controlling CD25 expression.

The fate of individual clones within the primary immune response is highly heterogeneous. Single antigen-specific $CD4^+$ precursor T cells can give rise to a clonally uniform T helper phenotype, but with a high amount of variability from clone to clone (14). This suggests that T helper fate decisions occur very early in the immune response, but that naive precursors T cells activated under similar *in vivo* conditions can give rise to highly distinct differentiation programs. Fate tracking of single $CD4^+$ T cell precursors and their progeny revealed heterogeneity in T helper differentiation even between precursor cells that expressed the same TCR (48). These results support our finding that differences in CD25 expression and ZAP-70 phosphorylation reflect heterogeneity in TCR signal strength even within a monoclonal T cell population. We speculate that the activity of TCR-mediated differentiation may be impacted and shaped by a number of environmental factors, including cytokines, costimulatory molecules, the APC and antigen dose. Future studies are required to determine the factors that can give rise to differential activation events among T cells even when the TCR is the same.

There are several limitations to the interpretation of this study. Although we report differences in TCR signal strength *in vitro*, it is important to note that the *in vitro* initiation of TCR signals may not fully predict the heterogeneity of the *in vivo* response. It is likely that *in vivo* activation results from multiple or prolonged contacts with antigen. Furthermore, *in vivo* activation may occur in microenvironments that have variable concentrations of

cytokines and other accessory signals. Our study does not distinguish between TCR signal strength and signal duration, and differences in antigen recognition by naïve T cells during the earliest phases of the immune response may have a distinct influence on memory formation as compared to antigen recognition by effector T cells during the peak of the infection, or in the late phases of the effector response. Additionally, TCR signaling is highly complex, and qualitatively distinct TCR signals may result from heterogeneity in antigen recognition during the polyclonal response. Future studies are needed to determine the impact of modulating multiple components of TCR signaling on $CD4^+$ memory T cell differentiation.

Materials and Methods

Design

The objective of this study was to explore the role of TCR signal strength in determining the differentiation of effector and memory $CD4^+$ T cells *in vivo*. Flow cytometry was used to assess the activation, differentiation and subsequent survival of $CD4^+$ T cells following acute viral infection within laboratory mice. Cellular analysis was performed during the early T cell effector phase, at the peak of the effector response and after memory formation. Techniques for the modulation of gene expression (shRNA) were used to confirm the results of observational studies. The sample size ($n = 3–5$) for the *in vivo* experiments was determined to be the optimal size for statistical analysis while using an appropriate number of laboratory mice and allowing for independent repeats. The investigators were not blinded when conducting or analyzing the experiments outlined in this study, the mice were randomly assigned to the different treatments and repeat experiments were carried out in both male and female cohorts, with no apparent sex differences.

Mice and Infections

C57BL/6 (6- to 8-weeks old) mice were purchased from Jackson Laboratories. SMARTA (49), Rag1-deficient, and SMα mice were maintained in our colony at the University of Utah. C7 and C26 mice were generated at the University of Utah Transgenic Core Facility by standard microinjection techniques using a T-cell-specific expression vector, VA-hCD2, in which the *Tcrb* gene was placed under the control of the human Cd2 promoter and a 3' locus control region of the *Cd2* gene (50). They were then bred with the previously generated SMα line (20) to produce a full TCR transgenic line on a $Tcra^{-/-}$ background. Mice are currently being back-crossed to a C57BL/6 background. LCMV Armstrong 53b was grown in BHK cells, titered in Vero cells, and injected intraperitoneally into recipient mice at a dose of 2×10^5 plaque-forming units. All mouse experiments were performed in accordance with protocols approved by the Institutional Animal Care and Use Committee at the University of Utah.

Cell Lines and retroviral transductions

We previously generated a panel of TCRs (20) cloned into MigR1. In this construct, the *TCRa* and *TCRb* sequences are separated by a cis-acting hydrolyzing element, P2A, that allows bicistronic expression (27) and possess an IRES-dependent mCherry reporter. Using previously described methods (28), replication incompetent retroviruses were used to

transduce the 58$\alpha^{-}\beta^{-}$ hybridoma cell line (23) expressing an NFAT reporter (hCD4-pA-GFP-NFAT-RV) (24) (provided by K. Murphy, Washington University, St. Louis, MO). The hybridoma lines were additionally transduced with a MigR1 retroviral construct expressing CFP under the control of NFκB minimal promoter (construct provided by P. Steinberger, Medical University of Vienna, Austria). Hybridoma lines were purified by FACS.

Cell Preparations and Flow Cytometry

Splenocyte and liver single cell suspensions were generated as previously described (8) and placed in cell culture media. Untouched $CD4^+$ T cells from SMARTA, C7, and C26 mice were isolated via magnetic beads (Miltenyi) and injected intravenously into B6 mice 1 day prior to LCMV infection. For cell-surface stains, single cell suspensions were incubated with fluorescently conjugated antibodies diluted in antibody staining buffer (PBS containing 1% FBS) at 4°C for 30–45 minutes. For intracellular cytokine assays, splenocytes were restimulated for 4 hours with 1μM $GP_{61–80}$ peptide from LCMV (GLKGPDIYKGVYQFKSVEFD) at 37°C in the presence of Brefeldin A (GolgiPlug, 1μl/ml), permeabilized with a kit (BD Biosciences) and stained with fluorescently labeled antibodies specific to the indicated cytokines. Transcription factor analysis was performed using Foxp3 Fixation/Permeabilization Buffer and accompanying protocol (eBioscience). To probe for phosphorylation events via flow cytometry, cells were immediately fixed after extraction from the animal and formation of a single cell suspension using pre-warmed (37°C) 1.5% PFA for 10 min at 37°C, followed by permeabilization in ice-cold 100% MeOH for 10 minutes. Cells were then incubated with antibodies to surface and intracellular targets 45–60 minutes. Tetramer staining was done for 1 hour at room temperature in RPMI containing 2% FBS and 0.1% sodium azide, followed by cell surface staining.

Retrogenic Bone Marrow Chimeras

To generate TCR retrogenic bone marrow chimeras, we used the above-described TCR expression constructs to generate retrovirus, then transduced TCR-expressing retroviruses into Rag1-deficient bone marrow cells using described methods (28). We then injected bone marrow cells intravenously into irradiated (450 rads) *Rag1*$^{-/-}$ hosts and monitored for the presence of $GFP^+TCR^+CD4^+$ T cells in the blood 8–10 weeks later.

Isolation of $CD25^{hi}$ and $CD25^{lo}$ early effector cells

C57BL/6 mice received 1–10 × 10^4 SMARTA $CD4^+$ T cells, followed 1 day later by LCMV infection. At day 3 or 5 post-infection, single cell splenocyte suspensions were stained with a non-depleting biotinylated anti-CD25 antibody (eBio7D4, eBioscience) (51) for 20 minutes on ice in MACS staining buffer (PBS with 0.5% BSA and 1 mM EDTA), followed by incubation with anti-Biotin MicroBeads (Miltenyi) for 20 additional minutes on ice. $CD25^{hi}$ and $CD25^{lo}$ $CD4^+$ T cells were separated via magnetic sorting columns (Miltenyi).

RNA Sequencing

$CD25^{hi}$ and $CD25^{lo}$ SMARTA $CD4^+$ T cells ($Thy1.1^+$) were FACS-sorted from splenocytes 5 days post LCMV infection. RNA was then extracted using a kit (miRNeasy, QIAGEN). Library preparation and RNA Sequencing performed by the University of Utah DNA

Sequencing Core Facility (NuGEN Ovation RNA-Seq System v2, HiSeq 50 Cycle Single Read) on a HiSeq 2000 (Illumina). Real Time Analysis Software (RTA v1.18.61) performed base calling and assigned a quality score to each base for each cycle. Reads were aligned to hg19 + splice junctions using NovoAlign. Spliced alignments were converted back to genomic space, sorted and indexed using Useq 8.8.9 SamTranscriptomeParser. Differentially expressed genes were determined using DefinedRegionDifferentialSeq (DRDS). Sequencing results were analyzed and differences in gene expression calculated by the University of Utah Bioinformatics Shared Resource. Sequencing raw data is available in the GEO repository (GSE114884).

RT PCR

RNA was isolated using TRIzol® (Life Technologies) and converted to cDNA using SuperScript III First Strand (Thermo Fischer). Semi-quantitative RT-PCR reactions were carried out using Power SYBR® Green PCR Master Mix (Life Technologies) and run on the LightCycler® 480 (Roche).

SHP-1 Knockdown

Retroviral vectors (pMig-R1) were used to express shRNA knockdown constructs specific for SHP-1 (SHP-1 KD) as previously described (47). A human microRNA (mir30) flanking sequence allowed for optimal expression and processing of siRNA (52). Knockdown was confirmed in EL-4 thymoma cell line. Knockdown in primary $CD4^+$ T cells was accomplished by transducing SMARTA bone marrow with SHP-1 KD or empty vector retrovirus and transplanting into irradiated *Rag1*$^{-/-}$ mice. Following reconstitution (8–10 weeks later), SMARTA $CD4^+$ T cells (GFP_+ and GFP^-) were then isolated from the spleen and transferred ($1–2 \times 10^4$) into B6 recipient mice that were subsequently infected with LCMV the next day. (53)

Statistical Analysis

Data analysis was performed using Prism (Graphpad) software.

Supplementary Material

Refer to Web version on PubMed Central for supplementary material.

Acknowledgements:

We acknowledge Tim Mosbruger and the Bioinformatics Shared Resource at the Huntsman Cancer Institute for assistance with deep sequencing and gene expression analysis. We acknowledge James Marvin and the University of Utah Flow Cytometry Core Facility for assistance with the design and execution of cell purification by FACS. We acknowledge the NIH Tetramer Core Facility for providing reagents.

Funding

Financial support for these studies was provided by the NIH (R01AI080830 and R01AI137248), the AAI Careers in Immunology Fellowship and the University of Utah.

Abbreviations

CFP	Cyan fluorescent protein
$GP_{61–80}$	glycoprotein 61–80 of LCMV
LCMV	lymphocytic choriomeningitis virus
MFI	mean fluorescence intensity
pepDC	peptide loaded dendritic cell
SHP-1	Src homology region 2 containing protein tyrosine phosphatase-1
KD	knockdown
EV	empty vector
pMHC	MHC Class II molecules presenting $GP_{61–80}$ peptide
pepDCs	dendritic cells presenting MHC Class II-restricted $GP_{61–80}$ peptide

References

1. Baruch EN, Berg AL, Besser MJ, Schachter J, Markel G, Adoptive T cell therapy: An overview of obstacles and opportunities. Cancer 123, 2154–2162 (2017). [PubMed: 28543698]
2. Bethune MT, Joglekar AV, Personalized T cell-mediated cancer immunotherapy: progress and challenges. Curr Opin Biotechnol 48, 142–152 (2017). [PubMed: 28494274]
3. Kaech SM, Wherry EJ, Heterogeneity and cell-fate decisions in effector and memory CD8+ T cell differentiation during viral infection. Immunity 27, 393–405 (2007). [PubMed: 17892848]
4. Williams MA, Bevan MJ, Effector and memory CTL differentiation. Annu Rev Immunol 25, 171–192 (2007). [PubMed: 17129182]
5. Huster KM, Busch V, Schiemann M, Linkemann K, Kerksiek KM, Wagner H, Busch DH, Selective expression of IL-7 receptor on memory T cell identifies early CD40L-dependent generation of distinct CD8+ memory T cell subsets. PNAS 101, 5610–5615 (2004). [PubMed: 15044705]
6. Marshall HD, Chandele A, Jung YW, Meng H, Poholek AC, Parish IA, Rutishauser R, Cui W, Kleinstein SH, Craft J, Kaech SM, Differential expression of Ly6C and T-bet distinguish effector and memory Th1 CD4(+) cell properties during viral infection. Immunity 35, 633–646 (2011). [PubMed: 22018471]
7. Obst R, van Santen HM, Mathis D, Benoist C, Antigen persistence is required throughout the expansion phase of a CD4(+) T cell response. J Exp Med 201, 1555–1565 (2005). [PubMed: 15897273]
8. Williams MA, Bevan MJ, Shortening the Infectious Period Does Not Alter Expansion of CD8 T Cells but Diminishes Their Capacity to Differentiate into Memory Cells. The Journal of Immunology 173, 6694–6702 (2004). [PubMed: 15557161]
9. Jelley-Gibbs DM, Brown DM, Dibble JP, Haynes L, Eaton SM, Swain SL, Unexpected prolonged presentation of influenza antigens promotes CD4 T cell memory generation. J Exp Med 202, 697–706 (2005). [PubMed: 16147980]
10. Brogdon JL, Leitenberg D, Bottomly K, The Potency of TCR Signaling Differentially Regulates NFATc/p Activity and Early IL-4 Transcription in Naive CD4+ T Cells. The Journal of Immunology 168, 3825–3832 (2002). [PubMed: 11937535]
11. Constant S, Pfeiffer C, Woodard A, Pasqualini T, Bottomly K, Extent of T Cell Receptor Ligation Can Determine the Functional Differentiation of Naive CD4+ T Cells. J Exp Med 182, 1591–1596 (1995). [PubMed: 7595230]

12. Choi YS, Yang JA, Yusuf I, Johnston RJ, Greenbaum J, Peters B, Crotty S, Bcl6 expressing follicular helper CD4 T cells are fate committed early and have the capacity to form memory. J Immunol 190, 4014–4026 (2013). [PubMed: 23487426]
13. Fazilleau N, McHeyzer-Williams LJ, Rosen H, McHeyzer-Williams MG, The function of follicular helper T cells is regulated by the strength of T cell antigen receptor binding. Nat Immunol 10, 375–384 (2009). [PubMed: 19252493]
14. Tubo NJ, Pagan AJ, Taylor JJ, Nelson RW, Linehan JL, Ertelt JM, Huseby ES, Way SS, Jenkins MK, Single naive CD4+ T cells from a diverse repertoire produce different effector cell types during infection. Cell 153, 785–796 (2013). [PubMed: 23663778]
15. Hwang S, Palin AC, Li L, Song KD, Lee J, Herz J, Tubo N, Chu H, Pepper M, Lesourne R, Zvezdova E, Pinkhasov J, Jenkins MK, McGavern D, Love PE, TCR ITAM multiplicity is required for the generation of follicular helper T-cells. Nat Commun 6, 6982 (2015). [PubMed: 25959494]
16. Ballesteros-Tato A, Leon B, Graf BA, Moquin A, Adams PS, Lund FE, Randall TD, Interleukin-2 inhibits germinal center formation by limiting T follicular helper cell differentiation. Immunity 36, 847–856 (2012). [PubMed: 22464171]
17. Pepper M, Pagan AJ, Igyarto BZ, Taylor JJ, Jenkins MK, Opposing signals from the Bcl6 transcription factor and the interleukin-2 receptor generate T helper 1 central and effector memory cells. Immunity 35, 583–595 (2011). [PubMed: 22018468]
18. Eto D, Lao C, DiToro D, Barnett B, Escobar TC, Kageyama R, Yusuf I, Crotty S, IL-21 and IL-6 are critical for different aspects of B cell immunity and redundantly induce optimal follicular helper CD4 T cell (Tfh) differentiation. PLoS One 6, e17739 (2011). [PubMed: 21423809]
19. Liao W, Lin JX, Wang L, Li P, Leonard WJ, Modulation of cytokine receptors by IL-2 broadly regulates differentiation into helper T cell lineages. Nat Immunol 12, 551–559 (2011). [PubMed: 21516110]
20. Kim C, Wilson T, Fischer KF, Williams MA, Sustained interactions between T cell receptors and antigens promote the differentiation of CD4(+) memory T cells. Immunity 39, 508–520 (2013). [PubMed: 24054329]
21. Moon JJ, Chu HH, Pepper M, McSorley SJ, Jameson SC, Kedl RM, Jenkins MK, Naive CD4(+) T cell frequency varies for different epitopes and predicts repertoire diversity and response magnitude. Immunity 27, 203–213 (2007). [PubMed: 17707129]
22. Williams MA, Ravkov EV, Bevan MJ, Rapid culling of the CD4+ T cell repertoire in the transition from effector to memory. Immunity 28, 533–545 (2008). [PubMed: 18356084]
23. Bäckström TB, Milia E, Peter A, Jaureguiberry B, Baldari CT, Palmer E, A motif within the T cell receptor α chain constant region connecting peptide domain controls antigen respo. Immunity 5, 437–447 (1996). [PubMed: 8934571]
24. Ise W, Kohyama M, Nutsch KM, Lee HM, Suri A, Unanue ER, Murphy TL, Murphy KM, CTLA-4 regulates pathogenicity of antigen-specific autoreactive T cells by cell-intrinsic and -extrinsic mechanisms. Nat Immunol 11, 129–135 (2010). [PubMed: 20037585]
25. Jutz S, Leitner J, Schmetterer K, Doel-Perez I, Majdic O, Grabmeier-Pfistershammer K, Paster W, Huppa JB, Steinberger P, Assessment of costimulation and coinhibition in a triple parameter T cell reporter line: Simultaneous measurement of NF-kappaB, NFAT and AP-1. J Immunol Methods 430, 10–20 (2016). [PubMed: 26780292]
26. van Panhuys N, Klauschen F, Germain RN, T-cell-receptor-dependent signal intensity dominantly controls CD4(+) T cell polarization In Vivo. Immunity 41, 63–74 (2014). [PubMed: 24981853]
27. Bettini ML, Bettini M, Vignali DA, T-cell receptor retrogenic mice: a rapid, flexible alternative to T-cell receptor transgenic mice. Immunology 136, 265–272 (2012). [PubMed: 22348644]
28. Holst J, Szymczak-Workman AL, Vignali KM, Burton AR, Workman CJ, Vignali DA, Generation of T-cell receptor retrogenic mice. Nat Protoc 1, 406–417 (2006). [PubMed: 17406263]
29. Kalia V, Sarkar S, Subramaniam S, Haining WN, Smith KA, Ahmed R, Prolonged interleukin-2Ralpha expression on virus-specific CD8+ T cells favors terminal-effector differentiation in vivo. Immunity 32, 91–103 (2010). [PubMed: 20096608]
30. Hondowicz BD, An D, Schenkel JM, Kim KS, Steach HR, Krishnamurty AT, Keitany GJ, Garza EN, Fraser KA, Moon JJ, Altemeier WA, Masopust D, Pepper M, Interleukin-2-Dependent

Allergen-Specific Tissue-Resident Memory Cells Drive Asthma. Immunity 44, 155–166 (2016). [PubMed: 26750312]

31. Hondowicz BD, Kim KS, Ruterbusch MJ, Keitany GJ, Pepper M, IL-2 is required for the generation of viral-specific CD4(+) Th1 tissue-resident memory cells and B cells are essential for maintenance in the lung. Eur J Immunol 48, 80–86 (2018). [PubMed: 28948612]
32. Schulz EG, Mariani L, Radbruch A, Hofer T, Sequential polarization and imprinting of type 1 T helper lymphocytes by interferon-gamma and interleukin-12. Immunity 30, 673–683 (2009). [PubMed: 19409816]
33. Woodrow M, Clipstone NA, Cantrell D, p21ras and Calcineurin Synergize to Regulate the Nuclear Factor of Activated T Cells. J Exp Med 178, 1517–1522 (1993). [PubMed: 8228805]
34. Martinez-Llordella M, Esensten JH, Bailey-Bucktrout SL, Lipsky RH, Marini A, Chen J, Mughal M, Mattson MP, Taub DD, Bluestone JA, CD28-inducible transcription factor DEC1 is required for efficient autoreactive CD4+ T cell response. J Exp Med 210, 1603–1619 (2013). [PubMed: 23878307]
35. Li JP, Yang CY, Chuang HC, Lan JL, Chen DY, Chen YM, Wang X, Chen AJ, Belmont JW, Tan TH, The phosphatase JKAP/DUSP22 inhibits T-cell receptor signalling and autoimmunity by inactivating Lck. Nat Commun 5, 3618 (2014). [PubMed: 24714587]
36. Brown DM, Kamperschroer C, Dilzer AM, Roberts DM, Swain SL, IL-2 and antigen dose differentially regulate perforin- and FasL-mediated cytolytic activity in antigen specific CD4+ T cells. Cell Immunol 257, 69–79 (2009). [PubMed: 19338979]
37. Crotty S, Johnston RJ, Schoenberger SP, Effectors and memories: Bcl-6 and Blimp-1 in T and B lymphocyte differentiation. Nat Immunol 11, 114–120 (2010). [PubMed: 20084069]
38. Ahlers JD, Belyakov IM, Matsui S, Berzofsky JA, Signals delivered through TCR instruct IL-12 receptor (IL-12R) expression: IL-12 and turmor necrosis factor-alpha synergize for IL-12R expression at low antigen dose. Int Immunol 13, 1433–1442 (2001). [PubMed: 11675375]
39. Watanabe N, Gavrieli M, Sedy JR, Yang J, Fallarino F, Loftin SK, Hurchla MA, Zimmerman N, Sim J, Zang X, Murphy TL, Russel JH, Allison JP, Murphy KM, BTLA is a lymphocyte inhibitory receptor with similarities to CTLA-4 and PD-1. Nat Immunol 4, 670–679 (2003). [PubMed: 12796776]
40. Safford M, Collins S, Lutz MA, Allen A, Huang CT, Kowalski J, Blackford A, Horton MR, Drake C, Schwartz RH, Powell JD, Egr-2 and Egr-3 are negative regulators of T cell activation. Nat Immunol 6, 472–480 (2005). [PubMed: 15834410]
41. Choi YS, Gullicksrud JA, Xing S, Zeng Z, Shan Q, Li F, Love PE, Peng W, Xue HH, Crotty S, LEF-1 and TCF-1 orchestrate T(FH) differentiation by regulating differentiation circuits upstream of the transcriptional repressor Bcl6. Nat Immunol 16, 980–990 (2015). [PubMed: 26214741]
42. Gullicksrud JA, Li F, Xing S, Zeng Z, Peng W, Badovinac VP, Harty JT, Xue HH, Differential Requirements for Tcf1 Long Isoforms in CD8(+) and CD4(+) T Cell Responses to Acute Viral Infection. J Immunol 199, 911–919 (2017). [PubMed: 28652395]
43. Shakya A, Goren A, Shalek A, German CN, Snook J, Kuchroo VK, Yosef N, Chan RC, Regev A, Williams MA, Tantin D, Oct1 and OCA-B are selectively required for CD4 memory T cell function. J Exp Med 212, 2115–2131 (2015). [PubMed: 26481684]
44. Hendriks J, Gravestein LA, Tesselaar K, van Lier RAW, Schumacher TNM, Borst J, CD27 is required for generation and long-term maintenance of T cell immunity. Nat Immunol 1, 433–440 (2000). [PubMed: 11062504]
45. Tanaka S, Tanaka K, Magnusson F, Chung Y, Martinez GJ, Wang YH, Nurieva RI, Kurosaki T, Dong C, CCAAT/enhancer-binding protein alpha negatively regulates IFN-gamma expression in T cells. J Immunol 193, 6152–6160 (2014). [PubMed: 25398328]
46. Plas DR, Johnson R, Pingel JT, Matthews RJ, Dalton M, Roy G, Chan AC, Thomas ML, Direct Regulation of ZAP-70 by SHP-1 in T Cell Antigen Receptor Signaling. Science 272, 1173–1176 (1996). [PubMed: 8638162]
47. Mahmood S, Kanwar N, Tran J, Zhang ML, Kung SK, SHP-1 phosphatase is a critical regulator in preventing natural killer cell self-killing. PLoS One 7, e44244 (2012). [PubMed: 22952938]

48. Cho YL, Flossdorf M, Kretschmer L, Hofer T, Busch DH, Buchholz VR, TCR Signal Quality Modulates Fate Decisions of Single CD4+ T Cells in a Probabilistic Manner. Cell Rep 20, 806–818 (2017). [PubMed: 28746867]

49. Oxenius A, Bachmann M, Zinkernagel RM, Hengartner H, Virus-specific MHC-class II-restricted TCR-transgenic mice: effects on humoral and cellular immune responses after viral infection. Eur J Immunol 28, 390–400 (1998). [PubMed: 9485218]

50. Zhumabekov T, Corbella P, Tolaini M, Kioussis D, Improved version of human CD2 minigene based vector for T cell-specific expression in transgenic mice. Journal of Immunological Methods 185, 133–140 (1995). [PubMed: 7665895]

51. Nihei J, Cardillo F, Dos Santos WL, Pontes-de-Carvalho L, Mengel J, Administration of a nondepleting anti-CD25 monoclonal antibody reduces disease severity in mice infected with Trypanosoma cruzi. Eur J Microbiol Immunol (Bp) 4, 128–137 (2014). [PubMed: 24883199]

52. Chen R, Belanger S, Frederick MA, Li B, Johnston RJ, Xiao N, Liu YC, Sharma S, Peters B, Rao A, Crotty S, Pipkin ME, In vivo RNA interference screens identify regulators of antiviral CD4(+) and CD8(+) T cell differentiation. Immunity 41, 325–338 (2014). [PubMed: 25148027]

53. Mora JR, Bono MR, Manjunath N, Weninger W, Cavanagh LL, Rosemblass M, von Andrian UH, Selective imprinting of guy-homing T cells by Peyer's patch dendritic cells. Nature 424, 88–93 (2003). [PubMed: 12840763]

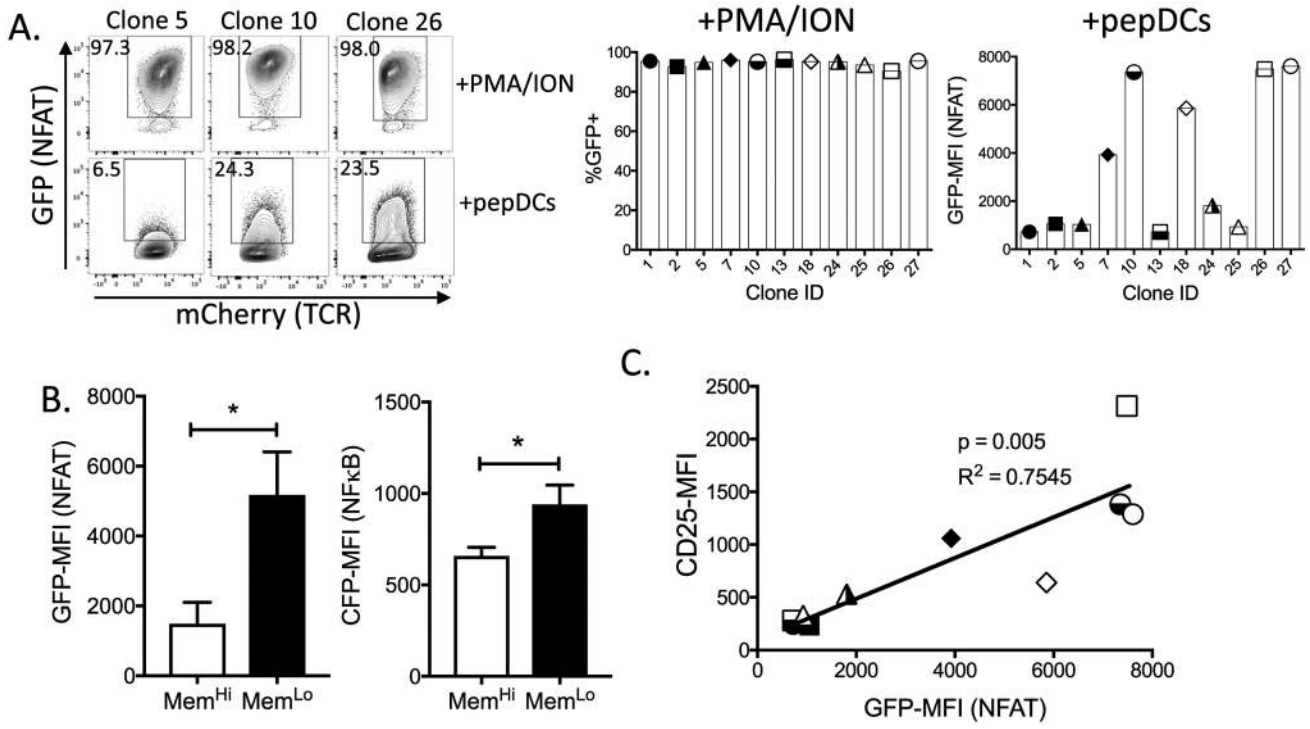

Fig. 1.

Memory-biased TCRs induce weaker TCR signals than effector-biased TCRs *in vitro*. **A)** Eleven T cell hybridoma lines, each expressing a unique $GP_{61–80}$-specific TCR, a NFAT GFP reporter and a NFκB CFP reporter were stimulated with $GP_{61–80}$-pulsed DCs (pepDCs) or PMA/Ionomycin for 24 hours. Representative flow plots show GFP expression for 3 of the cell lines. Bar graphs show GFP expression following stimulation with PMA/Ionomycin or pepDCs for 24 hours. **B)** Bar graphs depict GFP and CFP MFI following 24h stimulation, comparing TCRs that are present at reduced frequency at memory time points in vivo (Mem^{lo}) to TCRs that were present at equal or increased frequencies at memory time points (Mem^{hi}), as compared to the peak of the effector response. **C)** Plot indicates the correlation of GFP expression to either CD25 surface expression following 24 hour stimulation with pepDCs, as determined by Pearson's correlation. Throughout the study, error bars indicate the standard error of the mean (SEM), and statistical significance was determined by a Student's t test: *p < .05, **p < .01, ***p < .001. (n=3 biological replicates/group, representative of 3 independent experiments).

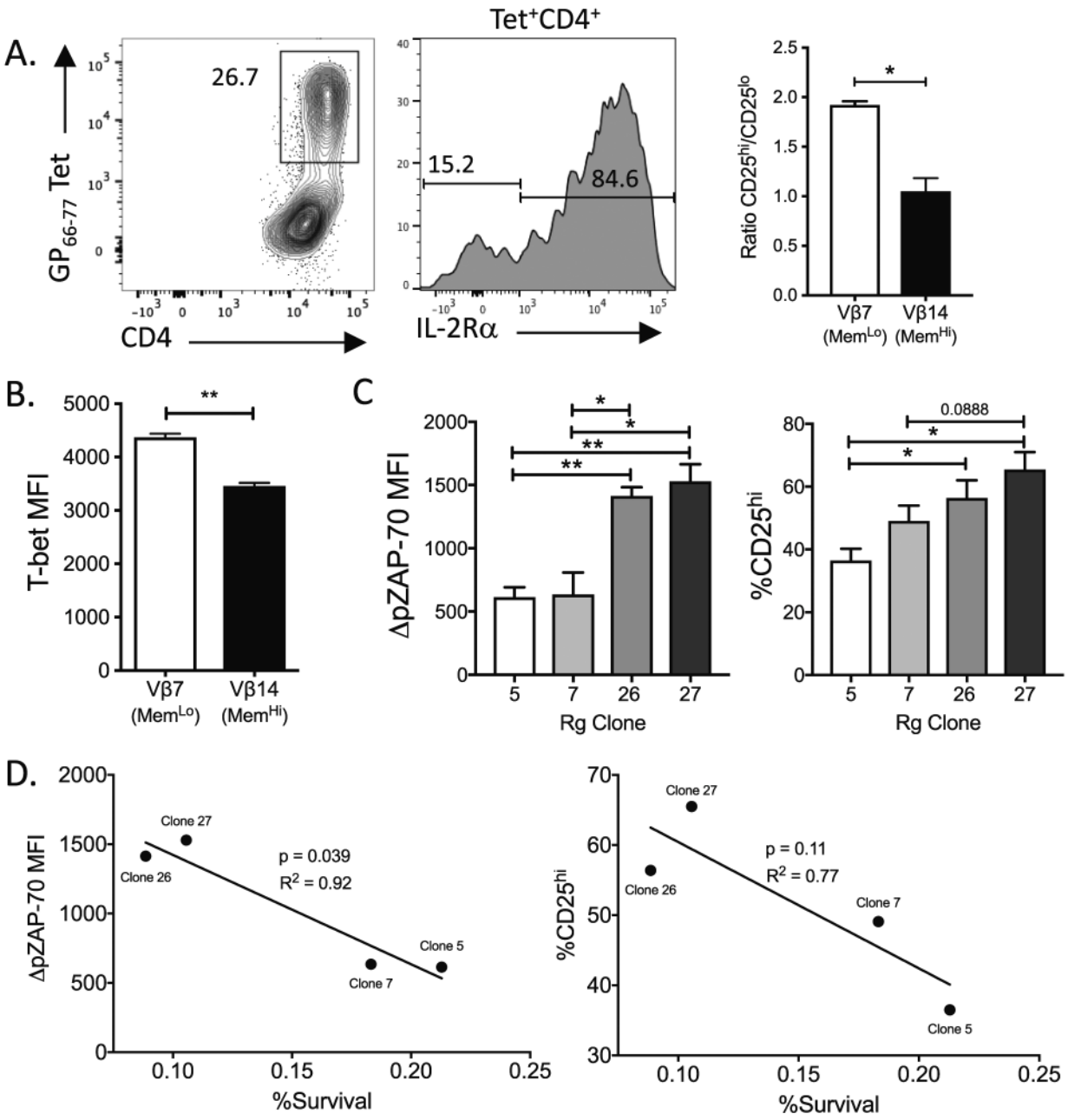

Fig. 2.

TCR signal strength and CD25 expression correspond to CD4$^+$ Tfh effector differentiation and memory T cell formation *in vivo*. **A)** At day 5 post-infection with LCMV, CD4$^+$ splenocytes from SMα mice were stained with I-A^b/GP$_{66–77}$ tetramer, CD25 and either Vβ7 or Vβ14. Representative plots show tetramer staining (gated on CD4$^+$) and CD25 staining (gated on CD4$^+$tetramer$^+$). The bar graph indicates the ratio frequency of Vβ7$^+$ or Vβ14$^+$ cells within the CD25^{hi} vs. CD25^{lo} tetramer$^+$ cells. **B)** Bar graph shows the T-bet MFI for Vβ7$^+$ and Vβ14$^+$ tetramer-binding cells. **C)** Four retrogenic (GFP$^+$) CD4$^+$ T cell lines were adoptively transferred (1×10^5 for analysis at day 3, $1–3 \times 10^4$ for analysis at days 8 and 42) into B6 hosts that were subsequently infected with LCMV. At day 3 post-infection, GFP$^+$ T

cells were analyzed for the presence of pZAP-70 and expression of CD25 by flow cytometry. The induction of ZAP-70 phosphorylation was calculated by subtracting the pZAP-70 MFI of the total $CD4^+$ T cell population from the pZAP-70 MFI of the GFP^+ Rg T cells (ΔpZAP-70). **D-E)** The numbers of GFP^+ retrogenic T cells in the spleen were calculated at days 8 and 42 post-infection, and percent survival between these two time points was calculated (% survival). The plots indicates the correlation of ΔpZAP-70 MFI (D) or CD25 expression (%$CD25^{hi}$)(E) at day 3 post-infection to % survival for each Rg TCR, as determined by Pearson's correlation. Error bars indicate the standard error of the mean (SEM), and statistical significance was determined by a Student's t test (n=3–5 mice/group, representative of at least 2 independent experiments).

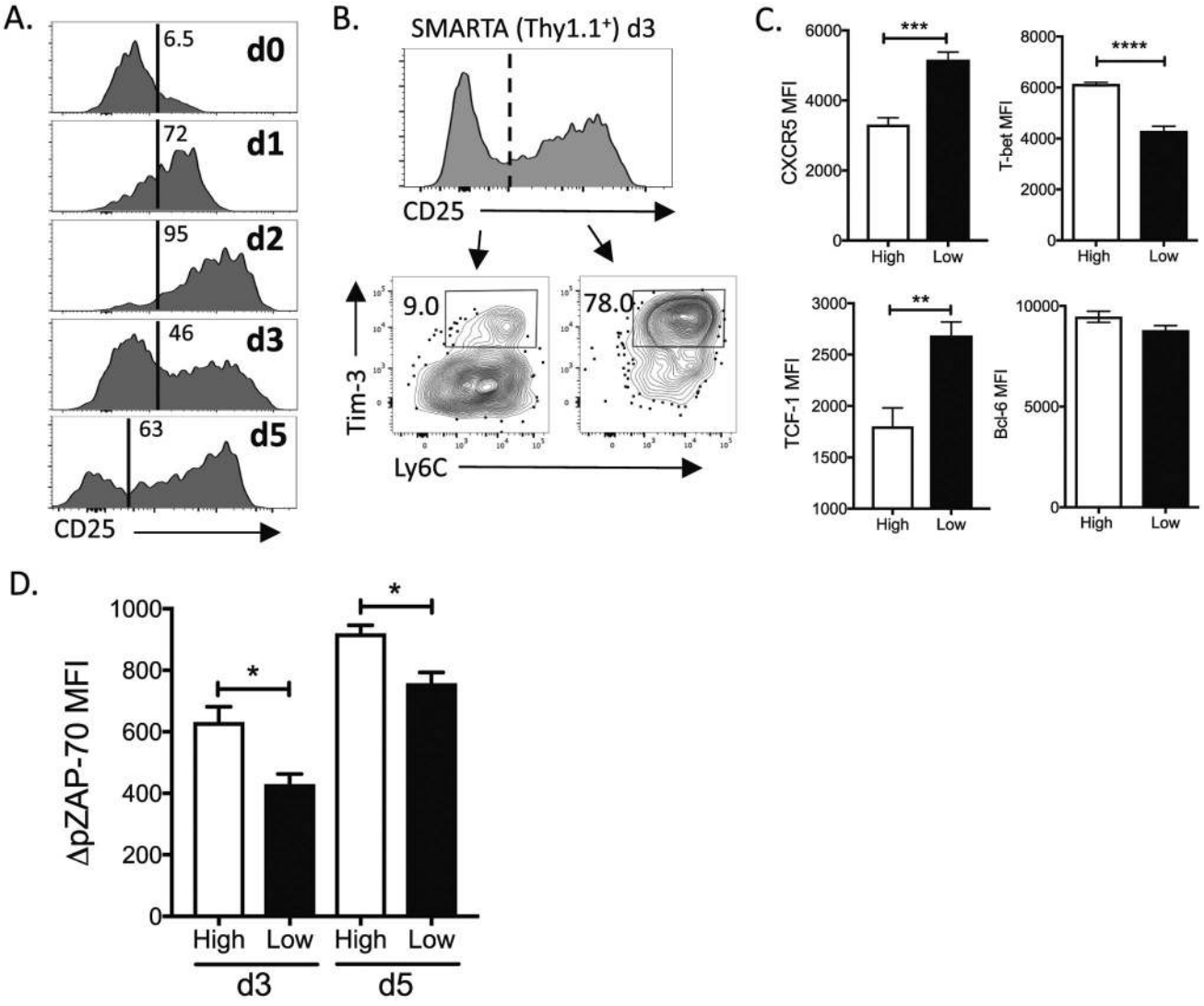

Fig. 3.

CD25 surface expression and TCR signal strength predicts T helper differentiation and memory potential of early effector T cells *in vivo*. **A)** SMARTA T cells (Thy1.1$^+$) were adoptively transferred (3×10^4) into B6 hosts (Thy1.2$^+$), followed by LCMV infection. Representative flow histograms indicate the CD25 surface expression by SMARTA T cells at days 0–5 after LCMV infection. **B)** The representative flow histogram shows expression of CD25 by SMARTA cells at day 3 post-infection and expression of Tim3 and Ly6C by CD25^{hi} and CD25^{lo} subsets. **C)** The bar graphs indicate the MFI of CXCR5, T-bet, TCF-1 and Bcl-6 in CD25^{hi} and CD25^{lo} SMARTA CD4$^+$ T cells in the spleen at d3 p.i., **D)** The bar graph indicates ΔpZAP-70 MFI of CD25^{hi} ("High") and CD25^{lo} ("Low") SMARTA CD4$^+$ T cells in the spleen at d3 and d5 post-infection. Error bars indicate the standard error of the mean (SEM), and statistical significance was determined by a Student's t test (n=4 mice/group, representative of four independent experiments).

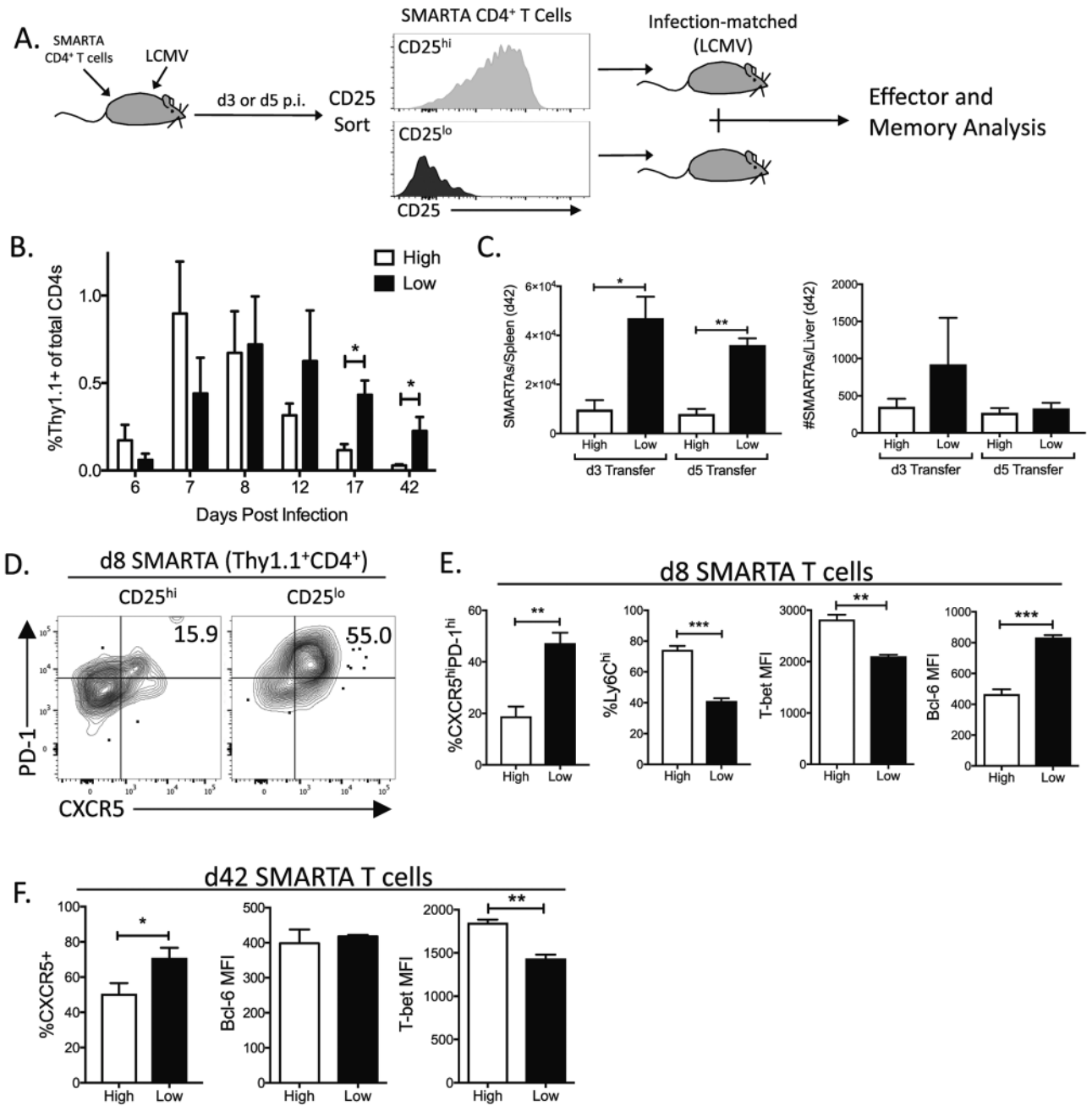

Fig. 4.

CD25 expression predicts effector and memory differentiation. **A)** Schematic depicts isolation and transfer of CD25^{hi} and CD25^{lo} early effector SMARTA CD4^{+} T cells infection matched secondary hosts. **B)** Graph indicates the frequency of SMARTA cells (Thy1.1^{+}) in the blood of secondary hosts at the indicated time points following transfer of CD25^{hi} ("High") and CD25^{lo} ("Low") SMARTA cells at d5 p.i. **C)** Bar graph indicates the total number of SMARTA memory cells (d42 p.i) in the spleen and liver following transfer of equal numbers of CD25^{hi} or CD25^{lo} early effector cells into infection-matched hosts at either d3 or d5 p.i. **D)** Plots indicate the frequency of CXCR5^{hi}PD-1^{hi} Tfh effector cells

derived from $CD25^{lo}$ and $CD25^{hi}$ effector SMARTA that were transferred at day 5 and analyzed at day 8. **E)** Bar graphs depict the frequency of Tfh ($CXCR5^{hi}PD\text{-}1^{hi}$) and Th1 ($Ly6C^{hi}$) day 8 effector cells derived from $CD25^{hi}$ and $CD25^{lo}$ early effector cells isolated and transferred at day 5 post-infection. Remaining bar graphs depict the MFI of Bcl-6 and T-bet at day 8. **F)** Bar graphs show the frequency of $CXCR5^{+}$ SMARTA cells in the spleen and the MFI following intracellular antibody staining for the presence of Bcl-6 and T-bet. Error bars indicate SEM, and statistical significance was determined by a Student's t test (n=3–5 mice/group, representative of at least 3 independent experiments).

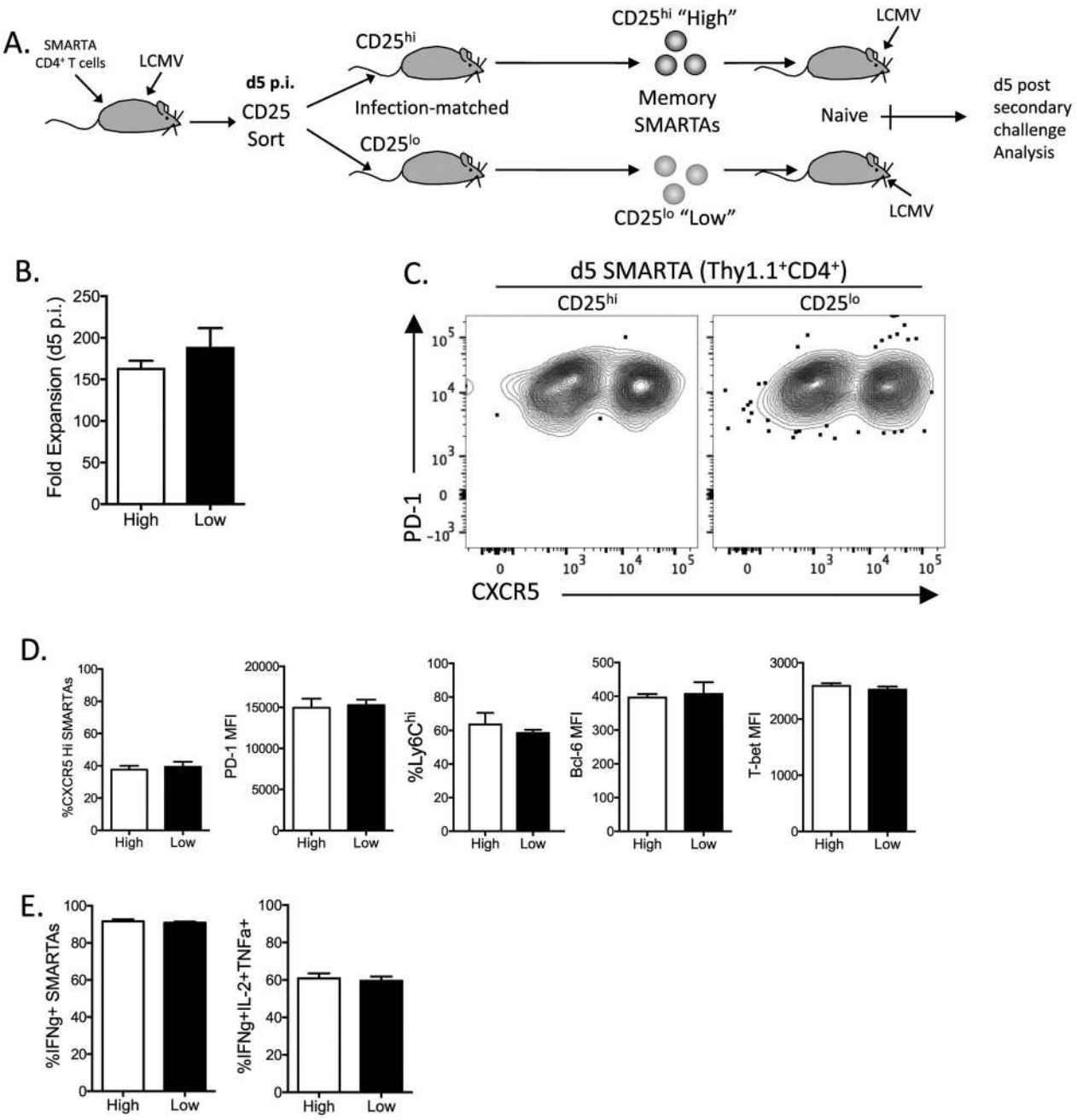

Fig. 5.

CD4+ memory T cells derived from either CD25hi or CD25lo effector cells respond robustly to secondary challenge. **A)** Schematic depicts the isolation and transfer of SMARTA memory cells (d42) derived from either d5 CD25hi or CD25lo effector populations into naïve B6 hosts, followed by secondary challenge with LCMV. **B)** Bar graph indicates the fold expansion of each SMARTA population as measured by splenic cell numbers at d5 post-secondary challenge. **C)** Representative flow plots show the expression of PD-1 and CXCR5 on SMARTA T cells 5 days after LCMV infection. **D)** Bar graphs indicate the expression levels of CXCR5, PD-1, Ly6C, Bcl-6 and T-bet in either frequency or MFI via flow

cytometry. **E)** Bar graphs show the frequency of single and multi-cytokine producing SMARTA T cells (d5 p.i.) following *ex vivo* peptide re-stimulation. Error bars indicate SEM, and statistical significance was determined by a Student's t test (n=3 mice/group).

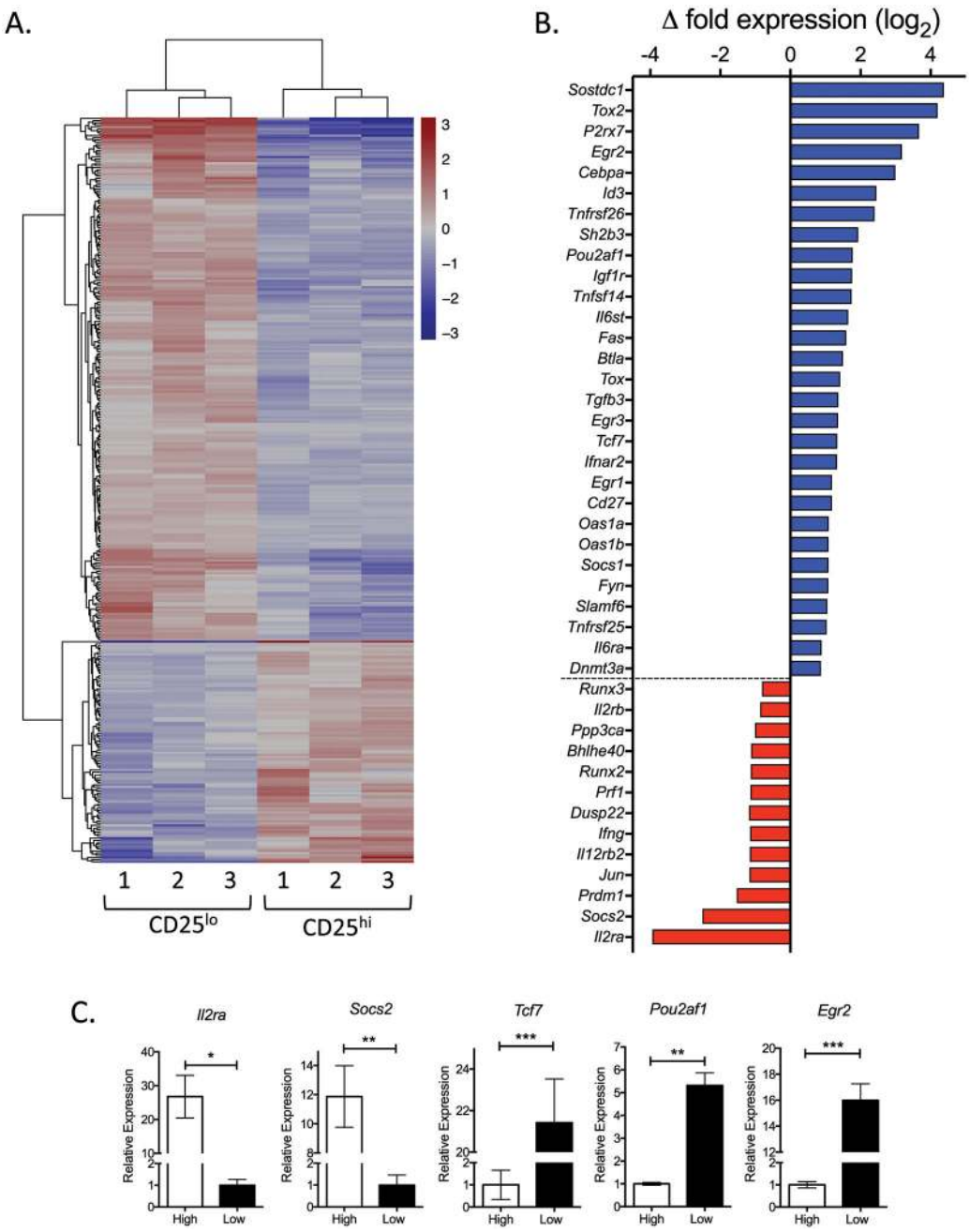

Fig. 6.

CD25 expression identifies two transcriptionally distinct subsets of very early effector cells. **A)** CD25^{hi} and CD25^{lo}SMARTA cells were isolated at d5 p.i. followed by RNASeq (n=3). Hierarchical clustering indicated unique gene expression patterns and significantly up-regulated (red) or down-regulated (blue) genes. **B)** Bar graph indicates a list of selected genes with significantly increased expression in CD25^{hi} (red) and CD25^{lo} (blue) populations. The x-axis indicates the difference in the number of transcripts on a log2 scale. **C)** Bar graphs show RT-PCR-based confirmation of differences in gene expression for the

selected genes between d5 $CD25^{hi}$ ("High") and $CD25^{lo}$ ("Low") SMARTA $CD4^{+}$ T cells. SEM (n=3 samples/group).

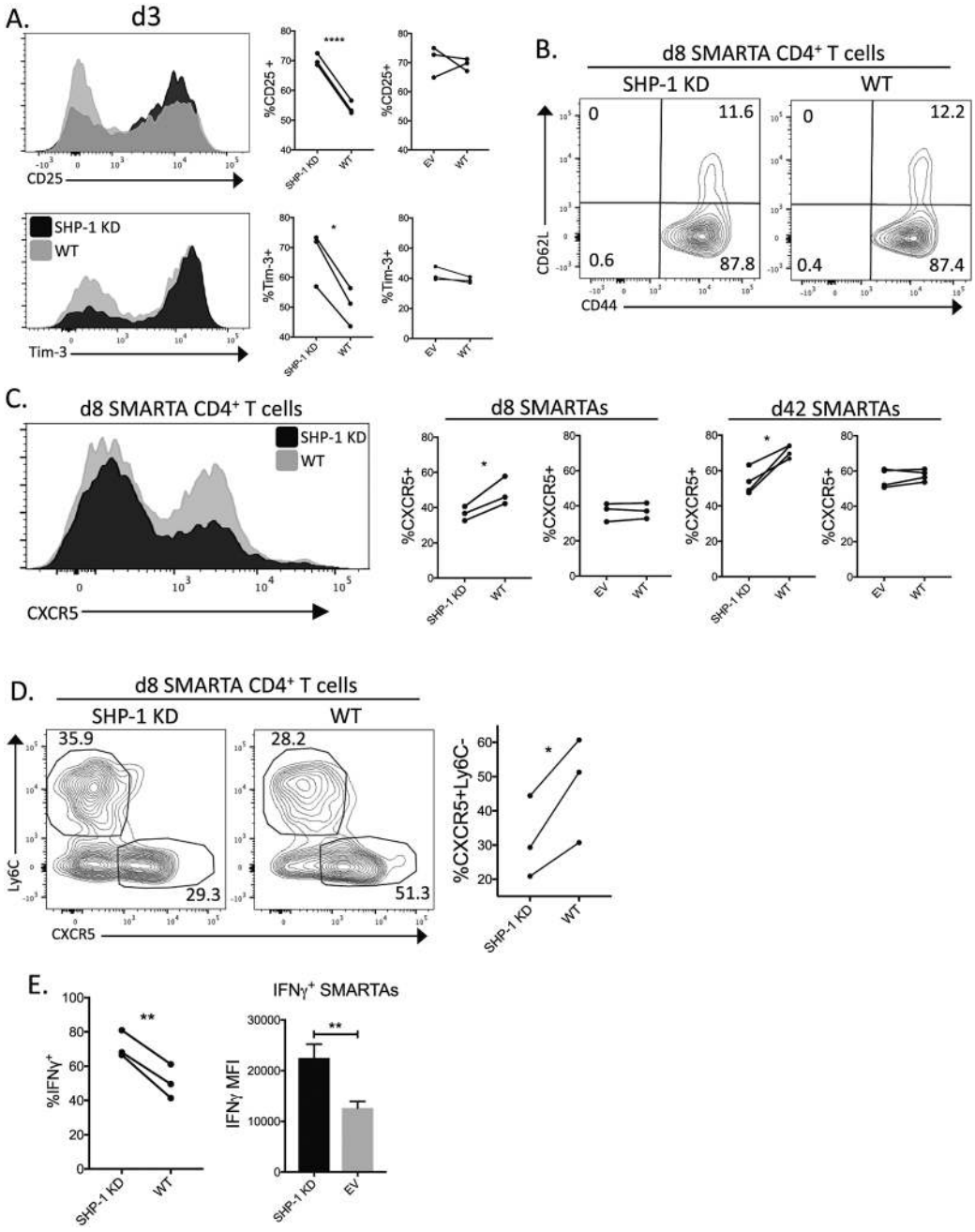

Fig. 7.

SHP-1 knockdown induces a bias towards effector and memory Th1 cells. We generated SMARTA bone marrow chimeras expressing either a SHP-1 specific shRNA or an empty vector control, along with a GFP reporter. At 8–10 weeks SMARTA T cells (Thy1.1$^+$) were adoptively transferred into B6 recipient and infected with LCMV. GFP$^+$ (SHP-1 KD or EV) and GFP$^-$ (non-transduced, WT) effector SMARTA cells from the spleen were analyzed. **A)** Representative flow plots show CD25 and Tim3 expression on SHP-1 KD (black) and WT (grey) SMARTA T cells 3 days post LCMV infection. Line graphs show the difference in the frequency of GFP$^+$ and GFP$^-$ SMARTA expressing each marker within the same mouse. **B)**

Representative flow plots show the surface expression of CD44 and CD62L on SMARTA T cells at d8 post infection. **C)** Representative flow histograms show CXCR5 expression by SHP-1 KD (GFP^+) and WT (GFP^-) SMARTA cells within the same mouse. Line graphs depict the differences in the frequency of CXCR5-expressing SMARTAs at d8 and d42 post-infection between GFP^+ and GFP^- SMARTA cells in the spleen in both SHP-1 KD and EV recipients. **D)** Representative flow plots show the expression of CXCR5 and Ly6C by SHP-1 KD (GFP^+) and WT (GFP^-) SMARTA cells in the spleen at day 8 post-infection. Numbers indicate the frequency of $CXCR5^+Ly6C^-$ (Tfh) and the $CXCR5^-Ly6C^+$ (Th1) SMARTA effector cells. The line graph shows the change of frequency of $CXCR5^+Ly6C^-$ SMARTA cells in the spleen when comparing SHP-1 KD (GFP^+) and WT (GFP^-) SMARTA in the same host. **E)** The line graph shows the change of frequency of IFNγ-secreting SMARTA cells in the spleen. The bar graph shows the IFNγ MFI of SHP-1 KD (GFP^+) and WT (GFP^-) SMARTA IFNγ-producing cells from the spleen. Error bars indicate the standard error of the mean (SEM). Pairwise comparisons and statistics were performed on GFP^+ and GFP^- SMARTA cells that were analyzed in the same recipient mouse. Results are representative of at least 2 independent experiments (n=3–4 mice/group).